

Global kinetic models for the oxidation of NO on platinum under lean conditions

W. Hauptmann^{a,*}, A. Drochner^a, H. Vogel^a, M. Votsmeier^b, and J. Gieshoff^b

^aDepartment of Technical Chemistry and Macromolecular Science, Darmstadt University of Technology, 64287 Darmstadt, Germany

^bUmicore AG & Co. KG, 63403 Hanau-Wolfgang, Germany

Different global kinetics for the oxidation of NO on platinum are compared in this work. The general form of the equation for the reaction rate is $r = k \cdot c_{NO}^\alpha \cdot c_{O_2}^\beta \cdot c_{NO_2}^\gamma \cdot TD^\delta$ with $TD = (1 - c_{NO_2} \cdot c_{NO}^{-1} \cdot c_{O_2}^{-0.50} \cdot K^{-1})$. Furthermore steady-state and temperature-programmed experiments were performed. The best results of simulation coupled with parameter estimation were obtained using $\alpha = 0.28$, $\beta = 0.49$, $\gamma = 0$ and $\delta = 1$, along with an activation energy of 47.5 kJ mol⁻¹.

KEY WORDS: diesel exhaust; NO oxidation; platinum; global model; monolithic catalyst.

1. Introduction

The NO-oxidation is an important step within the scope of exhaust gas after-treatment like NO_x storage reduction (NSR), the selective catalytic reduction (SCR) and the continuous regenerating trap (CRT) technologies. For modelling mainly elementary-like kinetic models are used [1–6]. The formation of NO₂ in the reaction networks is assumed to be of Eley–Rideal type [1–3] or Langmuir–Hinshelwood type kinetic [4–6], which sometimes even distinguishes between different catalytic sites for the reactants [5,6]. In addition to those elementary-like kinetic models a few global kinetic models have been published [7–9]. In contrast to the elementary-like kinetic models the reduced number of parameters in these equations facilitates handling of global kinetics, making them useful in modern motor management systems and for catalyst development. Unfortunately, these models are often limited to small ranges of validity. In this paper a comparison of global kinetics is given.

2. Experimental

A monolithic diesel oxidation catalyst (Umicore AG & Co. KG, Pt-loading: 80 g ft⁻³, washcoat: Al₂O₃/SiO₂, length: 7,62 cm, diameter: 2,54 cm, 400 cpsi) was tested under steady-state as well as transient conditions. The steady-state experiments were performed at different temperatures in a range between 373 and 643 K. For each temperature the NO-feed was varied between 75 and 450 vol-ppm while the O₂-fraction was held fixed at 6 vol-%. Additionally temperature-programmed (TP) experiments were performed from 353 to 643 K with a heating rate (β') of 5 K min⁻¹. Overall five different gas

compositions were tested (Table 1). The total flow was 965 L h⁻¹ resulting in a space velocity (SV) of 25 000 h⁻¹. N₂ was used as balance.

Before each experiment the catalyst was pre-treated at 643 K with 3 vol-% H₂ in N₂ for 1 h. The monolith was placed in a stainless steel plug-flow reactor (PFR) in a way the gas can't bypass the monolith. Before entering the monolith the gas was heated to the desired temperature. NO and NO_x were analysed using a chemiluminescence detector (CLD 822 S h, Eco Physics). The axial temperature profile was monitored using four K type thermocouples inserted into the monolith channels, filling and preventing flow through the channels. The impact on the flow field is assumed to be small since only 1% of the channels are blocked. Additionally the inlet gas temperature was measured 0.3 cm in front of the monolith. During the steady-state experiments the temperature change in the monolith was less than 1 K. For modelling purposes the catalyst temperature was used. The whole experimental setup is described in [10].

3. Kinetic models

To simulate the results of the steady-state and the TP-experiments a single channel simulator was used taking the mass and heat transfer between the bulk and the washcoat, mass and heat transfer in axial as well as in radial direction and the diffusion in the washcoat into account [11]. The reaction was assumed to take place only in the washcoat and the thickness of the washcoat was calculated to be 2.3×10^{-3} cm.

Different kinetic models were evaluated using this reactor model. The first, published by Marques *et al.* [7], was developed starting from a sequence of irreversible reactions leading to Eq. 1, with k being the rate constant and c_i being the concentration of species i .

* To whom correspondence should be addressed.
E-mail: hauptman@ct.chemie.tu-darmstadt.de

Table 1

Feed-gas compositions used for the TP-experiments (N ₂ as balance)	
NO/vol-ppm	O ₂ /vol-%
150	6
300	6
450	6
450	5
450	7

$$r = k \cdot c_{NO}^{0.30} \cdot c_{O_2}^{0.44} \quad (1)$$

For a NSR-catalyst Olsson *et al.* [8] used Eq. 2 to model the NO oxidation,

$$\begin{aligned} r &= k \cdot c_{NO} \cdot c_{O_2}^{0.50} - (k/K) \cdot c_{NO_2} \\ &= k \cdot c_{NO} \cdot c_{O_2}^{0.50} \cdot \left(1 - c_{NO_2} / \left(c_{NO} \cdot c_{O_2}^{0.50} \cdot K\right)\right) \end{aligned} \quad (2)$$

using the equilibrium constant K .

$$K = c_{NO_2,eq} / \left(c_{NO,eq} \cdot c_{O_2,eq}^{0.50}\right) \quad (3)$$

Here the reversibility of the NO oxidation is taken into account by adding the reverse reaction of NO₂. The first three factors on the right hand side of Eq. 2 can be interpreted as the kinetic part of Eq. 2 while the last factor provides for the deviation from the thermodynamic equilibrium.

Mulla *et al.* [9] published another kinetic model expressed in Eq. 4.

$$r = k \cdot c_{NO}^{1.05} \cdot c_{O_2}^{1.02} / c_{NO_2}^{0.92} \cdot \left(1 - c_{NO_2} / \left(c_{NO} \cdot c_{O_2}^{0.50} \cdot K\right)\right) \quad (4)$$

In contrast to Eq. 2 the NO₂ concentration is also considered to take the inhibiting effect of NO₂ into account. The thermodynamic part is identical to that used in Eq. 2.

Arrhenius equation was applied for expressing the rate constants. The activation energies (E_A) were taken from literature whereas all pre-exponential factors (A) were obtained by parameter estimation.

4. Results and discussion

For the steady-state experiments, the NO volume fractions ϕ_{NO} at the catalyst exit are shown in figure 1 in dependence of the NO inlet volume fractions. For clarity only four temperatures are plotted showing the main trends of these measurements. Evidently, the obtained curves can be divided into three different groups. The first is represented by the curve at 368 K and is characteristic for low temperatures. It shows a linear dependency on the feed-fraction, whereas the amount of

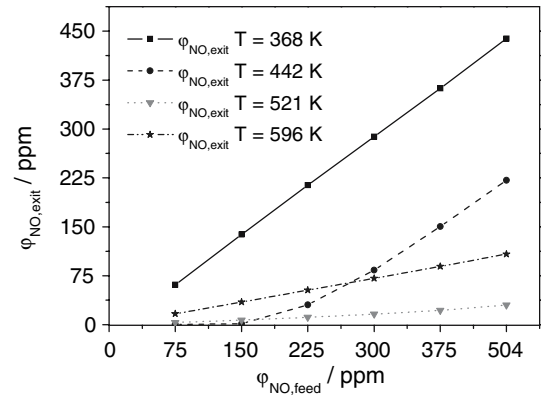


Figure 1. Results for steady-state experiments at different temperatures.

converted NO is independent from the inlet fraction. This factor, as well as a slope of one, indicates zero order of NO. A linear dependency on the feed-fraction is characteristic for temperatures above 596 K as well. For this temperature the slope is an exponential function of the residence time denoting a first order kinetic. It should be emphasised, that at this temperature the thermodynamic equilibrium is already reached and can therefore not be used to determine the kinetic parameters. For temperatures between 368 and 596 K, no linear dependency could be found. This indicates a reaction order of NO between 0 and 1.

These results agree well with those published by Després [12] who also found a temperature dependency of the reaction order for NO (0.30 at 423 K and 448 K, 0.36 at 473 K).

Figure 2 shows the conversion of NO as a function of the catalyst temperature for the TP experiment with 450 vol-ppm NO and 6 vol-% O₂. Also included in this figure are the results obtained using the published models.

As can be seen, the model published by Marques *et al.* [7] (Eq. 1) fits the experimental data best at low

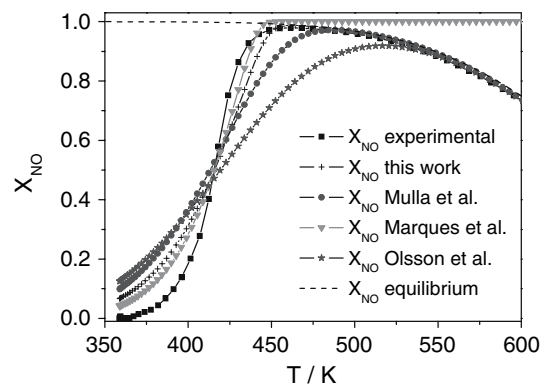


Figure 2. Calculated results compared to the NO conversion from a TP-experiment with a feed of 450 vol-ppm NO and 6 vol-% O₂ ($\beta' = 5 \text{ K min}^{-1}$, $SV = 25000 \text{ h}^{-1}$).

Table 2
Exponents used for Eq. 7

	α	β	γ	δ
Marques <i>et al.</i> [7]	0.30	0.44	0.00	0.00
Olsson <i>et al.</i> [8]	1.00	0.50	0.00	1.00
Mulla <i>et al.</i> [9]	1.05	1.03	-0.92	1.00
This work	0.28	0.49	0.00	1.00

temperatures. At high temperatures it predicts a total conversion of NO, which is contrary to the thermodynamic equilibrium. Eq. 2 (Olsson *et al.*) fits the experimental results at high temperatures. The maximum conversion is shifted to a higher temperature resulting in a lower value than determined experimentally. A better accuracy over the whole temperature range investigated here, can be obtained using Eq. 4 (Mulla *et al.*). But there is still some discrepancy between calculated and measured conversion especially at low temperatures.

A comparison of the three models shows, that all can be expressed using Eq. 5.

$$r = k \cdot c_{NO}^\alpha \cdot c_{O_2}^\beta \cdot c_{NO_2}^\gamma \cdot \left(1 - c_{NO_2} / \left(c_{NO} \cdot c_{O_2}^{0.50} \cdot K\right)\right)^\delta \quad (5)$$

To minimise the deviation between calculated and measured data the parameters were optimised. As described above, Mulla *et al.* added the NO₂ concentration to express the inhibiting effect of NO₂. In our opinion the inhibiting effect of NO₂ is based on platinum oxidation due to NO₂ [12,13]. The platinum oxidation is dependent on the amount of NO₂ and the actual oxidation state. But the actual oxidation state cannot be expressed using only the actual NO₂ concentration. Because of this the parameter γ is set to zero. Furthermore δ is set to one considering the thermodynamic part of Eq. 5. The parameter estimation was carried out for both the steady-state and the TP-experiments. For NO the reaction order obtained is 0.28 whereas the reaction order for O₂ is 0.49. The reaction order obtained by parameter estimation is in good accordance to those published by Després (0.30 at 423 K and 448 K, 0.36 at 473 K) [12] and Marques *et al.* (0.30) [7]. Furthermore it is consistent with the results

shown in figure 1. The reaction order for O₂ is also comparable to those published by Marques *et al.* (0.44) [7] as well as Olsson *et al.* (0.50) [8] and near the stoichiometric value of 0.5. But in this study O₂ was always used in great excess. Therefore, the influence of the O₂ concentration is small. The calculated curve using these parameters is also included in figure 2. For low temperatures the calculated conversion is too high as predicted by all the other models as well. But the discrepancies are much smaller than those created with Eq. 2 or 4, whereas the thermodynamic limitation is still predicted correctly.

For comparison table 2 shows the exponents used for all models.

The activation energy estimated here is 47.5 kJ mol⁻¹. A higher activation energy would lead to better fitting for the TP experiments but would cause bigger discrepancies for the steady-state experiments (not shown). This value is reasonable for the NO oxidation on platinum. Marques *et al.* determined the E_A to 57.7 kJ mol⁻¹ [7] while Olsson *et al.* used 39.2 kJ mol⁻¹ [8] which is almost identical with the value published by Mulla *et al.* (39 kJ mol⁻¹) [9]. With an excess of NO₂ in the feed Mulla *et al.* found 82 kJ mol⁻¹ [9] indicating an inhibition by NO₂.

The pre-exponential factor estimated for the TP experiments is 39 900 mol^{0.23} L^{-0.23} s^{-1.00}. To model the steady-state experiments the pre-exponential factor had to be decreased to 19 500 mol^{0.23} L^{-0.23} s^{-1.00}. This was necessary to follow the catalyst deactivation during the steady-state experiments. The reason for the deactivation is, that during the steady-state experiments the system had more time to form platinum oxides than in the TP-experiments.

Figure 3 shows the calculated results compared to the NO conversion from a TP-experiment with 150 and 300 vol-ppm NO.

The same tendencies as already shown in figure 2 can be seen in figure 3. Again less deviations between calculated and experimental results are obtained for the modified parameters (see Table 2).

All in all it should be emphasised, that all models show deviations between the calculated and the

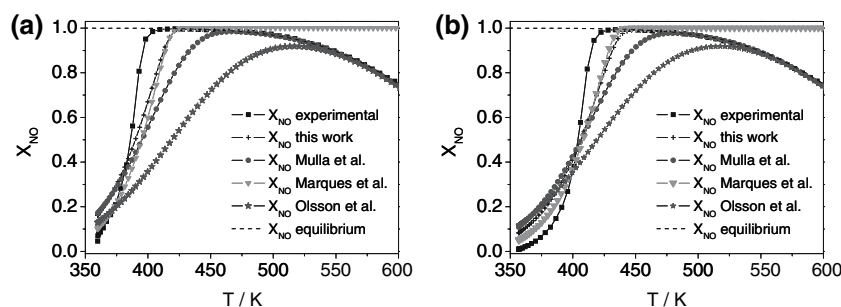


Figure 3. Calculated results compared to the NO conversion from a TP-experiment with a feed containing (a) 150 vol-ppm NO and (b) 300 vol-ppm NO (6 vol-% O₂, $\beta' = 5$ K min⁻¹, SV = 25000 h⁻¹).

experimental results. A complete description of the NO oxidation over the whole temperature range using these models is only conditionally possible. An improvement can be obtained by modifying the exponents, but still deviations exist, due to the simplicity of the global kinetic model. It only considers the thermodynamic equilibrium and does not take the catalyst deactivation, probably because of platinum oxidation [12,13] by NO₂, into account. Trying to do this by adding the NO₂ concentration to the kinetic part does not give better results. To improve the models a more accurate part for the catalyst deactivation should be investigated taking the catalyst history into account.

5. Summary

A comparative study between three already published global kinetic models for the NO oxidation was performed. To test these models, steady-state and temperature programmed experiments were carried out using a commercially available monolithic diesel oxidation catalyst. The models could all be expressed using Eq. 5 (see chapter 4). All models showed deviations between the calculated and experimentally obtained conversion. An optimisation of the reaction order resulted in smaller deviations. The reaction order for NO obtained during this optimisation process is 0.28 and the reaction order for O₂ is 0.49. The activation energy estimated here is 47.5 kJ mol⁻¹. One reason for the deviations is that the catalyst deactivation is not considered in this model. To consider the deactivation one has to take the history of the catalyst into account. This means that instead of a

global kinetic model a detailed elementary kinetic model should be used. But neglecting the catalyst deactivation offers the benefit of fewer parameters resulting in an easy to handle kinetic model. This low complexity also shortens the time needed for calculation. Therefore, it could be very useful to model CRT-, SCR- or NSR-aftertreatment systems for example or to obtain first approximations of the light-off temperature and the maximum conversion.

References

- [1] L. Olsson, B. Westerberg, H. Persson, E. Fridell, M. Skoglundh and B. Andersson, *J. Phys. Chem. B* 103 (1999) 10433.
- [2] M. Crocoll, PhD Thesis, Universität Karlsruhe (2003).
- [3] J.M.A. Harmsen, J.H.B.J. Hoebink and J.C. Schouten, *Catal. Lett.* 71 (2001) 81.
- [4] L. Olsson, H. Persson, E. Fridell, M. Skoglundh and B. Andersson, *J. Phys. Chem. B* 105 (2001) 6895.
- [5] X. Li, M. Meng, P. Lin, Y. Fu, T. Hu, Y. Xie and J. Zhang, *Top. Catal.* 22 (2003) 111.
- [6] H. Mahzoul, J.F. Brilhac and P. Gilot, *Appl. Catal. B* 20 (1999) 47.
- [7] R. Marques, P. Darcy, P. Costa, H. Mellottee, JM. Trichard and G. Djega-Mariadassou, *J. Mol. Catal. A: Chem.* 221 (2004) 127.
- [8] L. Olsson, R.J. Blint and E. Fridell, *Ind. Eng. Chem. Res.* 44 (2005) 3021.
- [9] S.S. Mulla, N. Chen, W.N. Delgass, W.S. Epling and F.H. Ribeiro, *Catal. Lett.* 100 (2005) 267.
- [10] S. Salomons, R. Hayes, M. Votsmeier, A. Drochner, H. Vogel, S. Malmberg, J. Gieshoff, *Appl. Catal. B* 70 (2007) 305.
- [11] L. Mukadi and R. Hayes, *Comp. Chem. Eng.* 26(3) (2002) 439.
- [12] J. Després, PhD Thesis, Diss. ETH No. 15006, ETH Zürich (2003).
- [13] L. Olsson and E. Fridell, *J. Catal.* 210 (2002) 340.